Supporting Information

Responsive Agarose Hydrogel Incorporating with Natural Humic Acid and MnO_2 Nanoparticles for Effective Relief of Tumor Hypoxia and Enhanced Photo-induced Tumor Therapy

Mengmeng Hou[a, b, 1], Weiwei Liu [c, 1], Lei Zhang [d], Leiyang Zhang [a], Zhigang Xu [a, b], Yang Cao [c, *], Yuejun Kang [a, b], Peng Xue [a, b, *]

[a] Key Laboratory of Luminescent and Real-Time Analytical Chemistry (Southwest University), Ministry of Education, School of Materials and Energy, Southwest University, Chongqing 400715, China.

[b] Chongqing Engineering Research Center for Micro-Nano Biomedical Materials and Devices, Chongqing 400715, China.

[c] Chongqing Key Laboratory of Ultrasound Molecular Imaging, Institute of Ultrasound Imaging, Second Affiliated Hospital, Chongqing Medical University, Chongqing, 400010, China.

[d] Institute of Sericulture and System Biology, Southwest University, Chongqing 400716, China.

[1] These authors contributed equally to this work.

Corresponding authors: xuepeng@swu.edu.cn (P. X), yangcao@cqmu.edu.cn (Y. Cao)

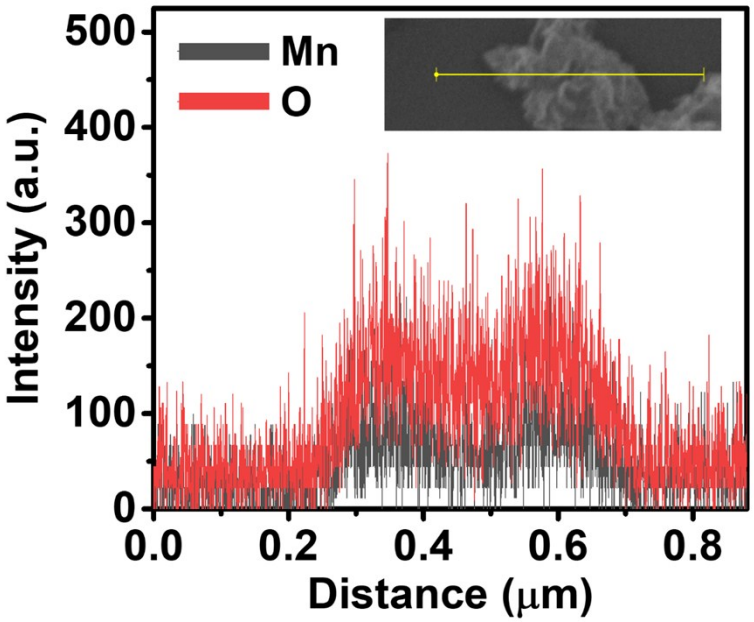

Fig. S1 Typical FESEM image of a single MnO_2 NP and linear scanning of the NP cross-section based on EDX analysis.

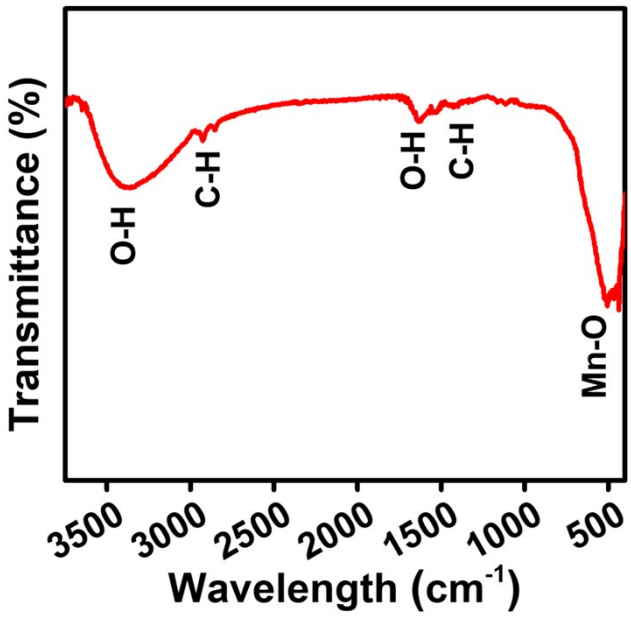

Fig. S2 FT-IR spectrum of MnO_2 NPs.

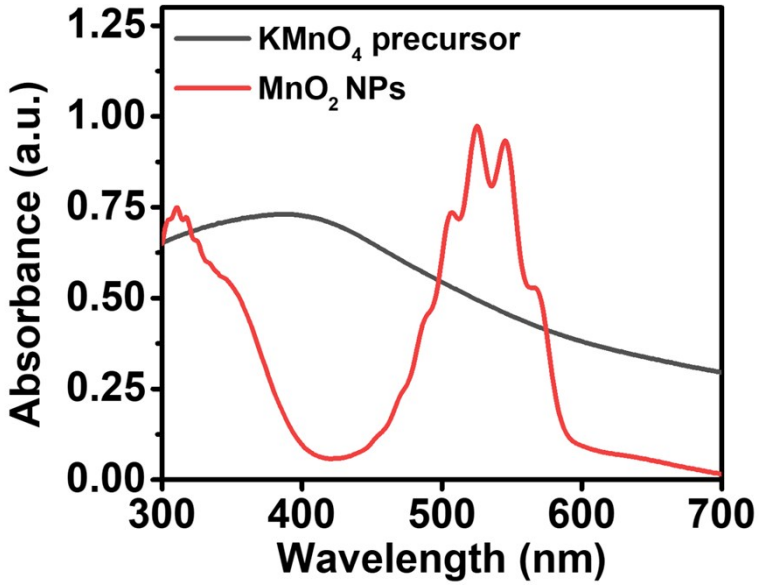

Fig. S3 UV-vis spectra of $KMnO_4$ precursor and as-developed MnO_2 NPs.

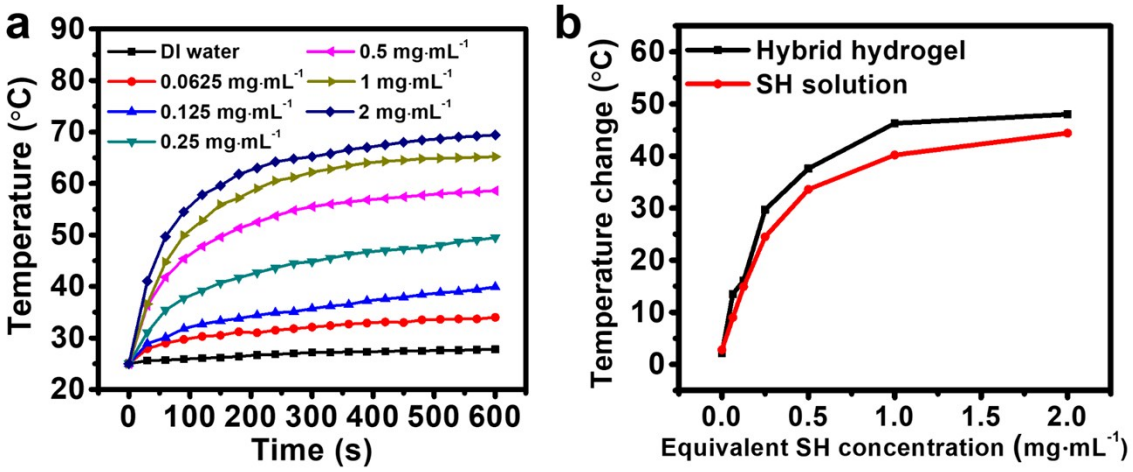

Fig. S4 (a) Temperature elevation of SH solution at various concentrations under NIR laser irradiation (808 nm, 1.5 $W \cdot cm^{-2}$) for 10 min; (b) Temperature elevation of SH solution or hybrid hydrogel after 10 min NIR laser irradiation under different equivalent SH concentrations.

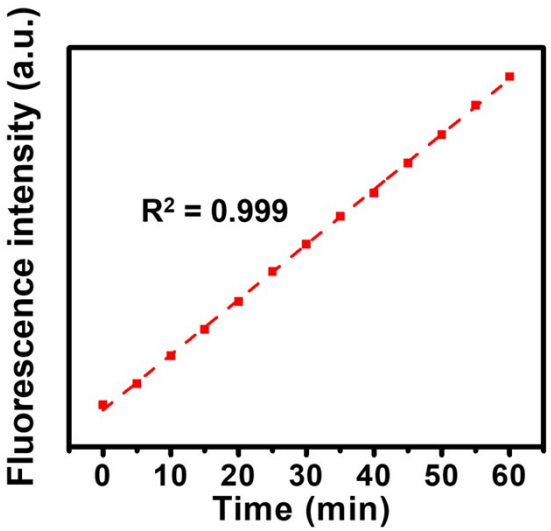

Fig. S5 Linear relationship between the peak fluorescence intensity (670 nm) and laser irradiation time corresponding to Fig. 3c (R^2=0.999).

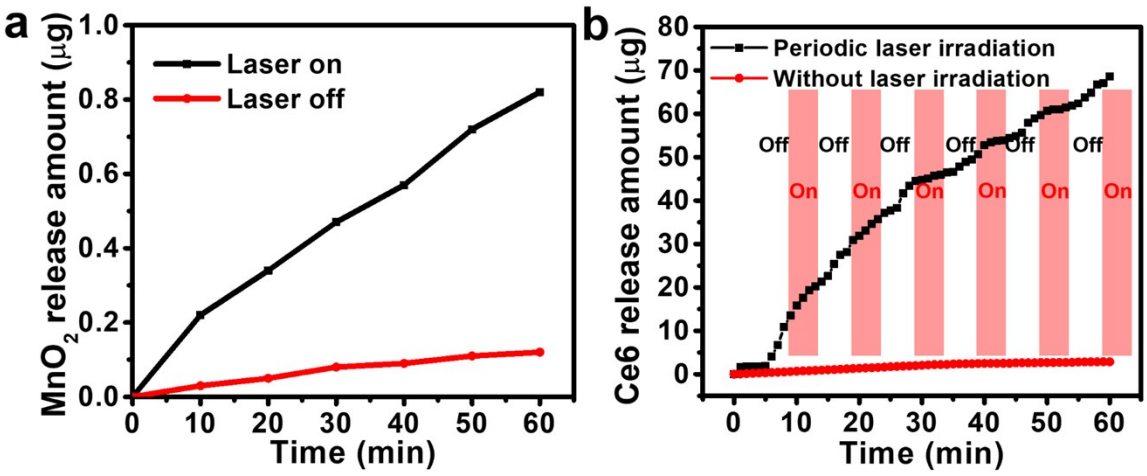

Fig. S6 (a) *In vitro* MnO_2 release from hybrid hydrogel under NIR laser irradiation or without any treatment; (b) cumulative Ce6 release from hybrid hydrogel under cyclic NIR laser irradiations or without any treatment (laser on: 5 min, laser off: 5 min per cycle).

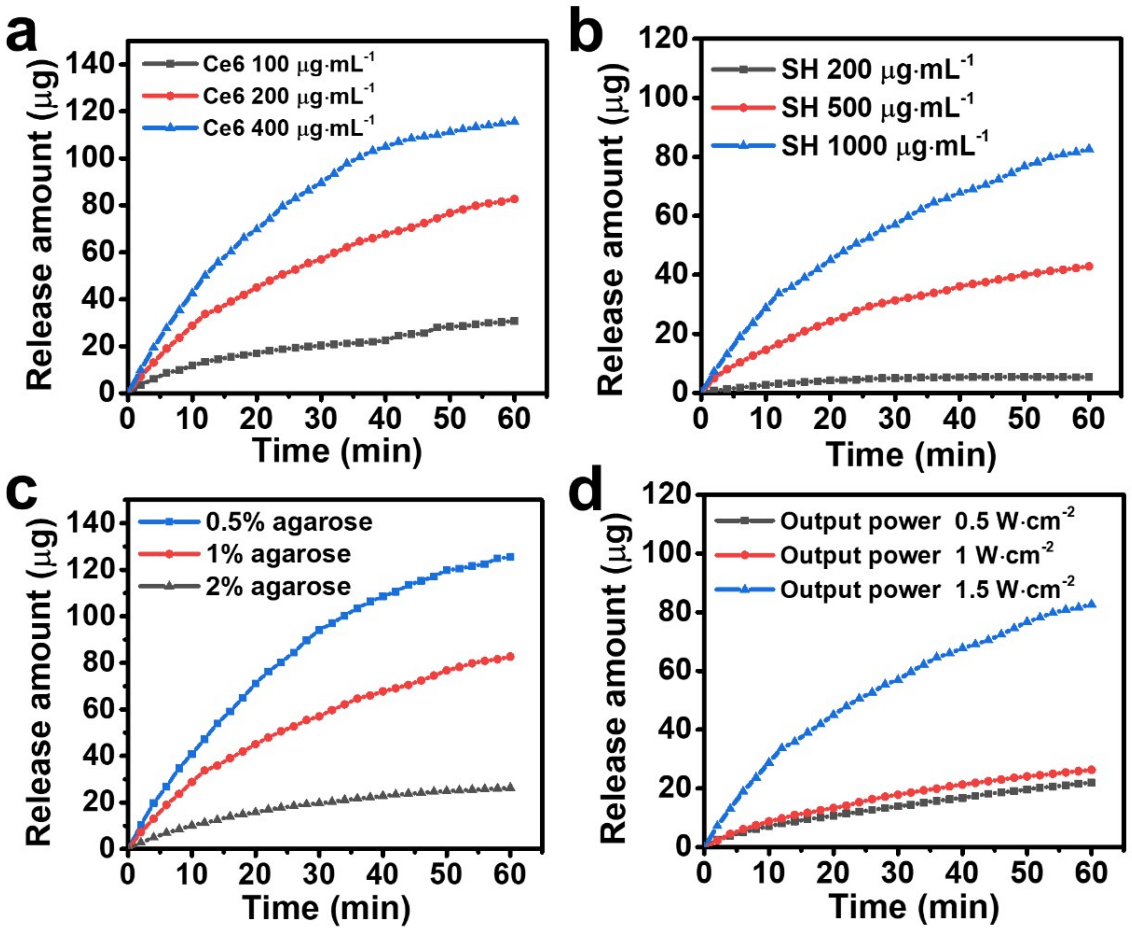

Fig. S7 Ce6 release from hybrid hydrogel by varying (a) Ce6 concentration (SH: 1000 μg·mL^{-1}, agarose: 1%, laser power 1.5 W·cm^{-2}), (b) SH concentration (Ce6: 200 μg·mL^{-1}, agarose: 1%, laser power 1.5 W·cm^{-2}), (c) agarose concentration (SH: 1000 μg·mL^{-1}, Ce6: 200 μg·mL^{-1}, laser power 1.5 W·cm^{-2}) and (d) laser power (Ce6: 200 μg·mL^{-1}, SH: 1000 μg·mL^{-1}, agarose: 1%).

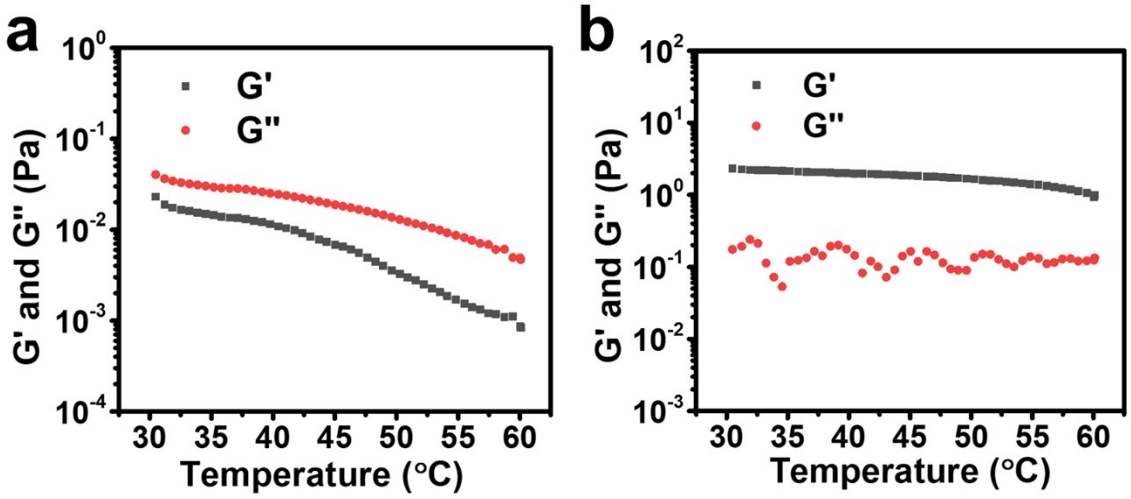

Fig. S8 Oscillatory shear rheology (G' and G") of the hybrid hydrogel prepared from (a) 0.5% and (b) 2% agarose displayed in temperature-dependent modulus.

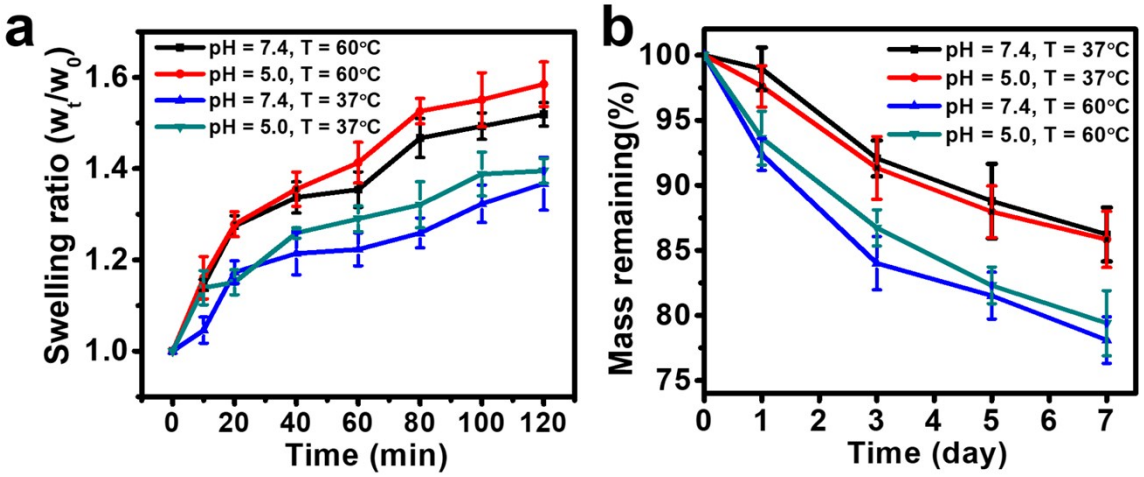

Fig. S9 Degradation of hybrid hydrogel in 1×PBS under different pH conditions (pH = 5.0 and 7.4) and environmental temperatures (T = 37°C and 60°C) by calculating (a) the swelling ratio of hydrated hydrogel and (b) the weight of reserved freeze-dried hydrogel over time.

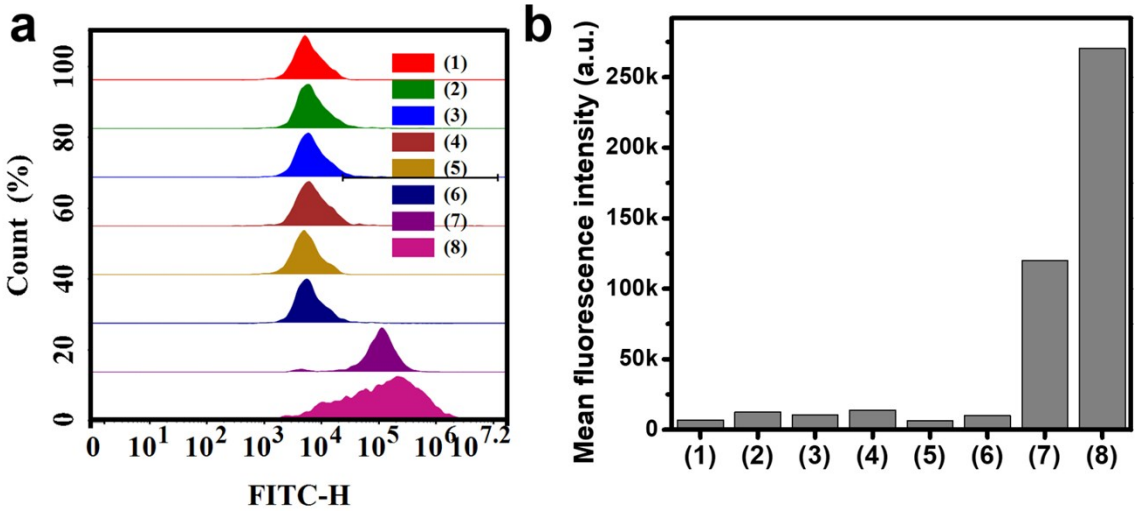

Fig. S10 Flow cytometry analysis of (a) cell count vs. log of normalized DCF fluorescence and (b) mean intensity of DCF fluorescence emission corresponding to Fig. 5c. Group 1: Blank; group 2: H_2O_2; group 3: Agarose@SH/Ce6 + H_2O_2; group 4: Hybrid hydrogel + H_2O_2; group 5: Blank + Laser; group 6: H_2O_2 + Laser; group 7: Agarose@SH/Ce6 + H_2O_2 + Laser; group 8: Hybrid hydrogel + H_2O_2 + Laser.

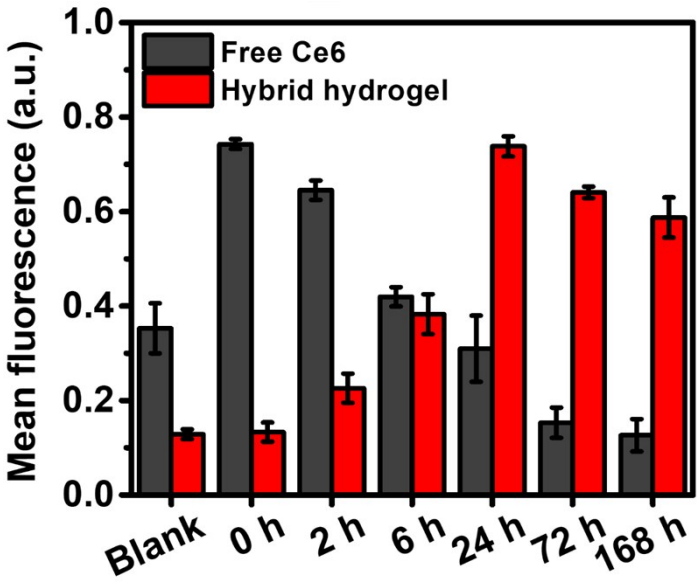

Fig. S11 Mean fluorescence intensity in tumor region at different time intervals corresponding to Fig. 7d.

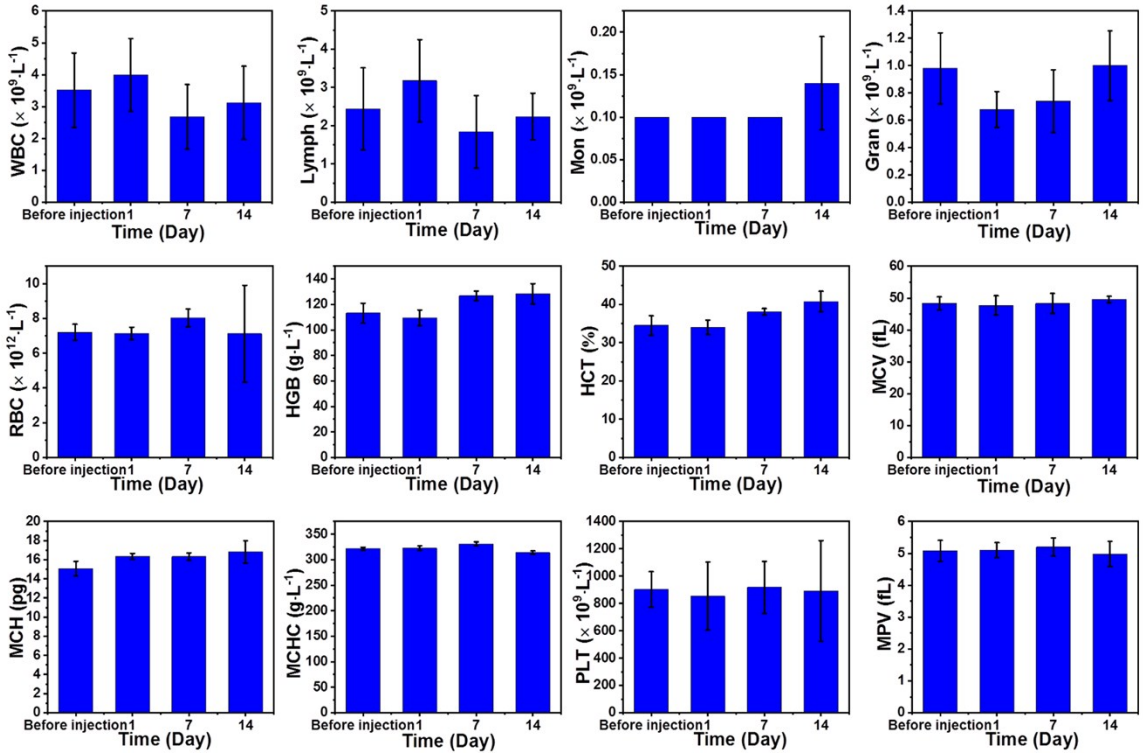

Fig. S12 Complete blood count at various time points after tumor bearing BALB/c mice being intratumorally injected with hybrid hydrogel.

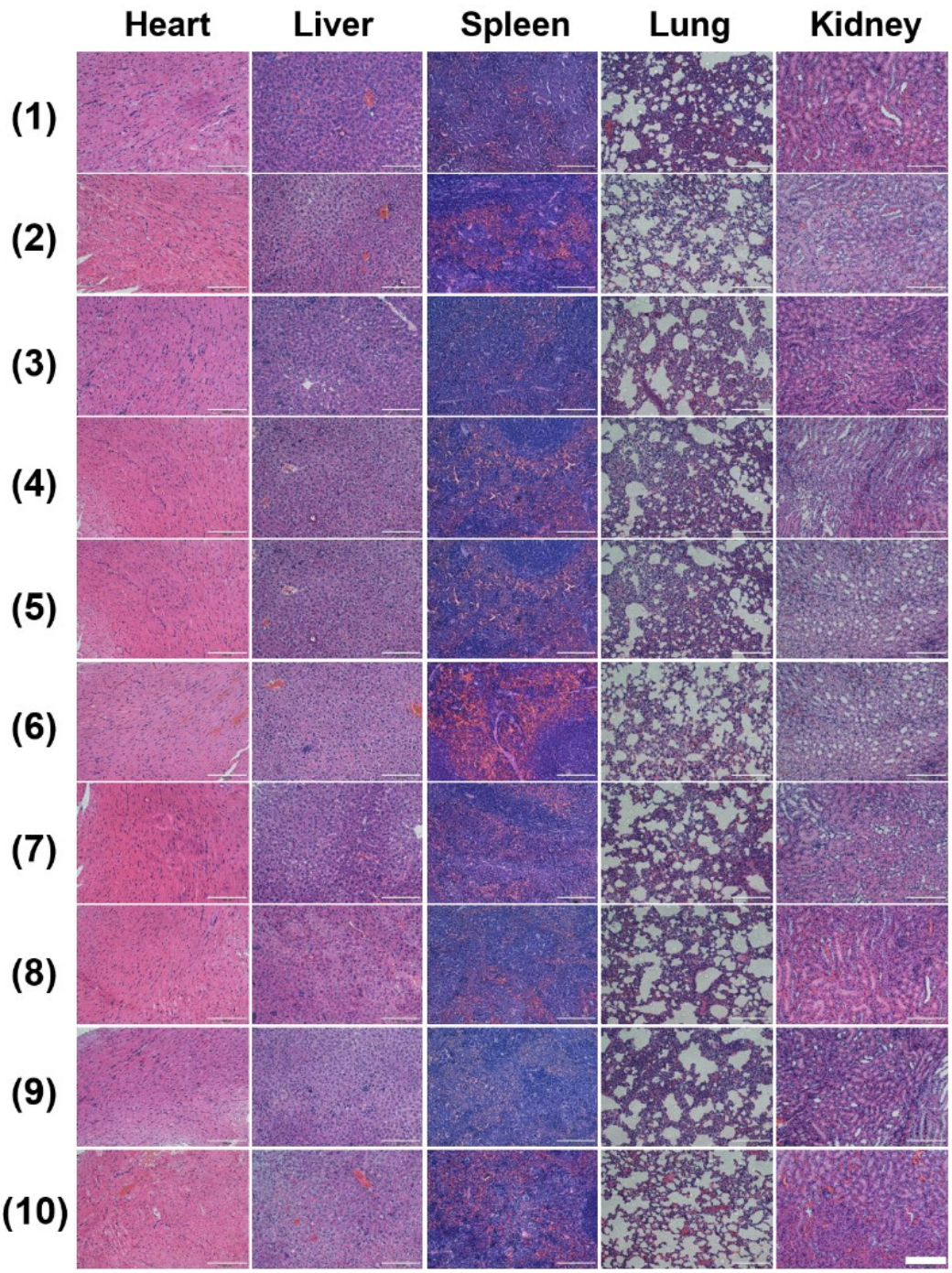

Fig. S13 Histological analysis of the sections excised from major organs through H&E staining on day 14 post-injection (scale bars: 200 μm).

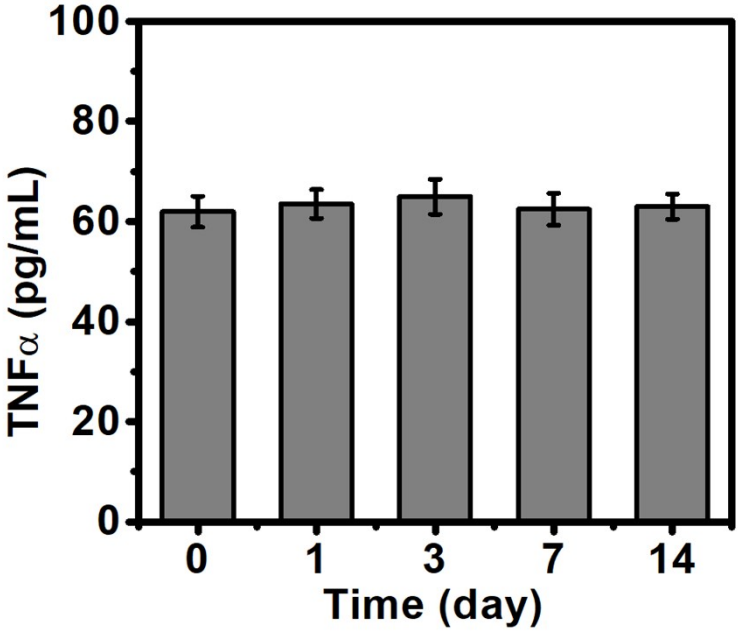

Fig. S14 Level of TNF-α in peripheral blood of mice after intratumoral injection with hybrid hydrogel (50 μL for each).